Journal of *Marine Science and Engineering*

MDPI

Review

Creep Behavior Research of Deep-Sea Pressure Hull: A Review

Yuan Zeng [1,2], Changli Yu [2,*] and Shuo Yang [2]

[1] School of Civil Engineering, Harbin Institute of Technology, Harbin 150090, China; 24b333002@stu.hit.edu.cn
[2] School of Ocean Engineering, Harbin Institute of Technology (Weihai), Weihai 264209, China; yangshuo@hit.edu.cn
* Correspondence: yuchangli@hitwh.edu.cn

Abstract: Pressure hulls are the primary pressure-bearing structures in submersibles and deep-sea space stations, which are essential for marine scientific research. Due to repeated dive cycles and extended operational periods, these hulls undergo creep deformation over time, posing risks to their structural integrity. This paper provides a comprehensive review of research on the creep behavior of pressure hulls, focusing on three key aspects: creep testing, creep constitutive models, and numerical simulation techniques. Initially, various creep testing methodologies are presented, with the experimental data serving as a foundational basis for subsequent analyses. Experimental data from creep tests form the foundation for constructing and validating constitutive models, which are critical for predicting long-term deformation. The review also explores advanced numerical simulation techniques, such as user subroutines and multiscale modeling, to analyze creep in complex pressure hull structures. Finally, based on the insights from the reviewed studies, the paper proposed potential directions for future research to address current challenges and enhance the design and maintenance of pressure hulls.

Keywords: creep; pressure hull; creep test; constitutive models; numerical simulation

1. Introduction

With the increasing exploration and utilization of marine resources, the development of marine engineering equipment has advanced significantly. Among these, deep-sea submersibles are indispensable tools in marine scientific research. The pressure hull, as the core structural component of a submersible, directly withstands external pressures and ensures operational safety. Throughout its service life, a submersible undergoes repeated dive cycles and prolonged operation in extreme deep-sea environments, making it subjected to repeated high-pressure loads, resulting in cumulative creep deformation over time. In addition, in the future deployment of a deep-sea space station, the pressure hull will endure long-term sustained hydrostatic pressure, resulting in creep behavior.

Creep is the time-dependent strain increase in solids under constant load, occurring even below the yield limit, unlike plastic deformation. This process degrades material strength and stability, redistributing stress within structures. For pressure hulls, accounting for creep behavior during design is essential to ensure long-term safety.

Research on pressure hull creep behavior focuses on three interrelated aspects: creep testing, constitutive modeling, and numerical simulation (see Figure 1). Creep testing directly measures material creep characteristics. These data inform mathematical models that relate creep to factors like time and temperature, yielding constitutive models. Numerical simulations then use these models to analyze creep in diverse structural designs.

check for updates

Received: 12 March 2025
Revised: 4 April 2025
Accepted: 7 April 2025
Published: 8 April 2025

Citation: Zeng, Y.; Yu, C.; Yang, S. Creep Behavior Research of Deep-Sea Pressure Hull: A Review. *J. Mar. Sci. Eng.* **2025**, *13*, 749. https://doi.org/10.3390/jmse13040749

Copyright: © 2025 by the authors. Licensee MDPI, Basel, Switzerland. This article is an open access article distributed under the terms and conditions of the Creative Commons Attribution (CC BY) license (https://creativecommons.org/licenses/by/4.0/).

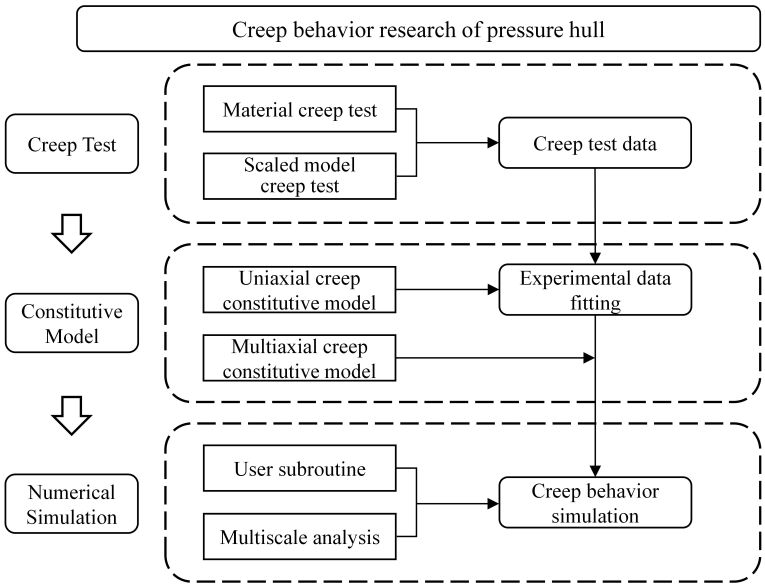


Figure 1. Flowchart for the creep behavior research of pressure hulls.

This review is organized as follows. Section 2 summarizes two types of creep tests: material creep tests and structural creep tests. Section 3 introduces several commonly used uniaxial creep constitutive models, comparing their applicability across different scenarios. Additionally, modified constitutive models and multiaxial creep constitutive models are discussed. Section 4 focuses on numerical simulation methods, including user subroutines and multiscale methods, to simulate the creep behavior of isotropic and anisotropic materials. Finally, the paper outlines future research directions for studying the creep behavior of pressure hulls.

2. Creep Test

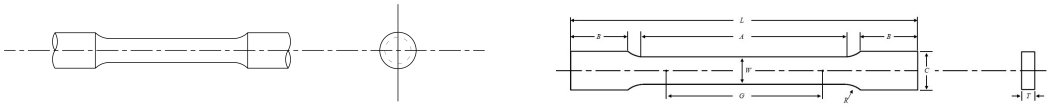
Creep testing is a crucial method for studying the creep behavior of pressure hulls and obtaining material creep parameters. These tests are divided into two types: material creep tests and structural creep tests. Material creep tests, the primary approach, involve preparing samples according to standards and applying creep loading to determine material parameters. Structural creep tests use full-ocean-depth simulation devices to apply long-term pressure on scaled or full-scale pressure hull models. Strain data collected during these tests reveal the structural creep behavior.

2.1. Material Creep Tests

Material creep tests were conducted on titanium alloy and polymethyl methacrylate (PMMA) to investigate their creep properties. Titanium alloy, known for its high specific strength and excellent corrosion resistance, is widely used in marine engineering equipment. It is a primary material for the pressure hulls of manned deep-sea submersibles capable of full-depth scientific exploration [1]. PMMA, characterized by low density, high transparency, strain-rate strengthening, and high strain-rate embrittlement, is commonly used as a visual window in manned submersibles. In recent years, PMMA has also gained popularity as a material for the pressure structures of manned cabins in submersibles operating at depths of up to 2000 m.

Material creep tests involve preparing tensile or compressive specimens, applying creep loading, and collecting strain data using extensometers or similar equipment to generate strain–time curves for analyzing creep behavior. The American Society for Testing and Materials (ASTM) provides standardized guidelines for such tests, including ASTM E139-11 (2018) [2] for metals and ASTM D2990-17 [3] for plastics. Specimen shapes are

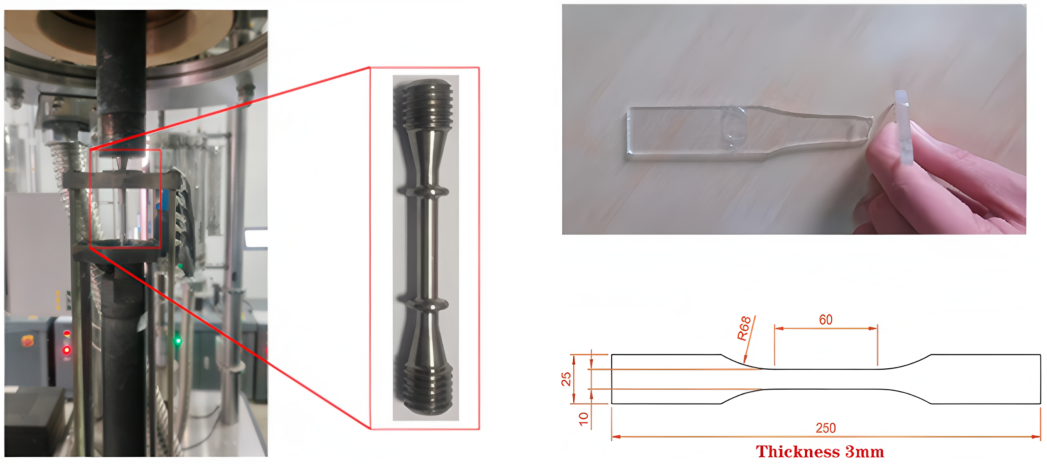
typically circular or rectangular, as illustrated in Figure 2, with specific requirements for testing equipment. Creep loading is commonly applied using a universal testing machine or a dedicated creep testing machine [4–7]. Similarly, GB/T 2039-2024 [8] and GB/T 15048-1994 [9], the national standards of China, provide provisions for uniaxial tensile creep tests on metals and compressive creep tests on plastics.



(**a**) (**b**)

Figure 2. Specimen material creep tests [10]: (**a**) round cross-section specimen; (**b**) rectangular cross-sectional specimen.

Tensile creep tests are more commonly conducted than compression creep tests due to their simpler operation. Given that modern pressure hulls typically utilize isotropic metal materials or organic glass, research has predominantly focused on tensile creep tests. Chen J. [11] conducted tensile creep tests at room temperature on a novel titanium alloy used for pressure hulls. Using an electronic creep fatigue testing machine, cylindrical specimens were subjected to creep loading under seven different stress levels for 48 h. The resulting strain–time curves and performance indices, such as yield strength and tensile strength, were obtained. Liu et al. [12] performed multiple room-temperature tensile creep tests on cylindrical specimens of Ti-6Al-4V and Ti-6Al-2V titanium alloys (see Figure 3a), generating creep curves under four different stress levels. Similarly, Liu et al. [13] conducted four sets of tensile creep tests on PMMA samples (see Figure 3b) to investigate the creep damage behavior of submersible windows. The tests provided creep parameters for PMMA under pressures equivalent to a water depth of 3000 m.



(**a**) (**b**)

Figure 3. Tensile creep specimen: (**a**) tensile creep specimen of titanium alloy [12]; (**b**) tensile creep specimen of PMMA [13].

With the growing demand for lightweight structures and enhanced strength in pressure hulls, fiber-reinforced resin matrix composites are increasingly utilized due to their excellent corrosion resistance, high specific strength, and high specific modulus. As anisotropic materials, these composites exhibit pronounced tension–compression asymmetry. For pressure hulls subjected to compressive loads, it is essential to conduct compression creep tests to accurately determine the creep characteristics of material.

The research methodology for investigating the compressive creep behavior of fiber-reinforced composites is similar to that used for tensile creep tests on titanium alloys [14–18].

Axial compressive loads are typically applied using material testing machines to obtain the material's creep characteristics. However, creep testing specifically for composite pressure hulls remains limited, highlighting the need for further research in this area.

2.2. Creep Test of Pressure Hull Scale Models

Creep testing of pressure hull scale models (see Figure 4) is primarily conducted to investigate parameters such as the stress threshold for creep and to analyze the impact of creep behavior on the structural safety performance. These experiments utilize ultra-high-pressure equipment to simulate deep-sea environments. However, such tests are time-intensive and constrained by the operational capacity of the equipment, resulting in limited research in this area. In existing studies, test pressures are often set as multiples of the maximum working pressure of pressure hull, such as the maximum working pressure or 1.25 times this value. This approach enables researchers to accelerate the observation of creep characteristics within a shorter timeframe.



(**a**) (**b**)

Figure 4. Scaled model of pressure hull: (**a**) cylindrical pressure hull [18]; (**b**) spherical pressure hull [19].

Wang et al. [19] conducted a creep test on a titanium alloy spherical pressure hull scale model with an inner diameter of 300 mm and a thickness of 30 mm, as shown in Figure 4b, using ultra-high-pressure experimental equipment. The test maintained a maximum working pressure of 115 MPa for 160 h. Following unloading, the pressure was increased to 130 MPa for 620 h, then unloaded and raised to 144 MPa for 160 h. The results indicate that the model experienced compressive creep only at 1.25 times the maximum working pressure (144 MPa). In this high-stress condition, the strain rate of the model approaches a constant.

Stachiw et al. [20] conducted pressure tests on a scaled model of an acrylic spherical pressure hull at six different pressure levels over a duration of 1 h. Their study revealed that both the creep rate and cumulative creep increase exponentially with pressure. This increased creep accumulation was found to reduce the buoyancy of the spherical pressure hull.

The high time and economic costs associated with creep tests on scaled models, combined with the difficulty of directly correlating experimental data to the creep behavior of pressure hulls in specific working environments, have limited research in this area.

3. Creep Constitutive Model

A creep constitutive model describes the relationship between strain and time under long-term constant stress or load. It is developed based on extensive experimental data. Using creep test results, the strain–time curve, known as the creep curve, can be plotted. A typical creep curve is shown in Figure 5, illustrating three distinct phases. The primary creep phase is characterized by a continuously decreasing creep rate. In the secondary creep phase, the creep rate remains nearly constant, so it is called the steady-state creep phase. This phase represents the minimum creep rate of the material, and the material's resistance to creep can be evaluated based on this phase. As a result, it is the most extensively studied phase. The tertiary creep phase exhibits a rapidly increasing creep rate, leading to accelerated deformation and eventual material failure. Since the creep behavior varies across these phases, distinct constitutive models have been developed to describe each phase.

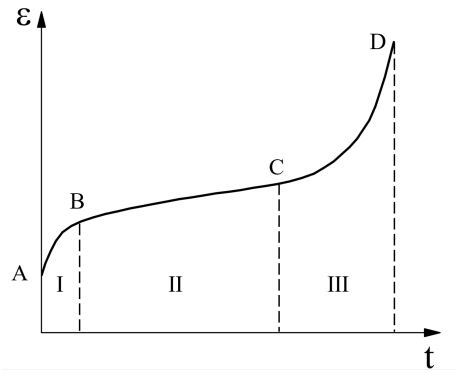


Figure 5. Typical creep curve.

Given the complex stress field experienced by structures in working environments, creep models can be categorized into uniaxial and multiaxial models based on the type of stress, such as uniaxial or multiaxial stress conditions. The following sections introduce commonly used uniaxial and multiaxial creep models in the study of pressure hulls.

3.1. Uniaxial Creep Constitutive Model

Existing research primarily establishes uniaxial creep constitutive models using the macroscopic phenomenological approach, based on creep testing, to describe the material creep phenomenon at a macroscopic level [21–26]. The creep behavior of materials is influenced by stress, time, and temperature, which could be simulated by the following Equation [27]:

$$\varepsilon_{cr} = F(\sigma, T, t) = f(\sigma)g(T)h(t) \tag{1}$$

where ε_{cr} is creep strain, σ is stress, T is temperature, and t is time.

Norton Model and Its Variants

Equation (1) leads to the development of various creep constitutive models, including the Norton model [28], Norton–Bailey model [29], Graham model [30], Garofalo model [31], and others. The Norton model, which involves fewer parameters, is commonly used to describe the secondary creep phase:

$$\dot{\varepsilon}_{cr} = A\sigma^n \tag{2}$$

where A and n are material constants and $\dot{\varepsilon}_{cr}$ is creep strain rate.

When considering the temperature effect, the Norton model can be written in the general form shown in Equation (3) [32]:

$$\dot{\varepsilon}_{cr} = C_1 \sigma^{C_2} e^{-C_3/T} \tag{3}$$

Building on this, by incorporating the time hardening effect, the time hardening model, as shown in Equation (4), can be derived. If the strain hardening effect is considered, the strain hardening model, as shown in Equation (5), can be obtained:

$$\dot{\varepsilon}_{cr} = C_1 \sigma^{C_2} t^{C_3} e^{-C_4/T} \tag{4}$$

$$\dot{\varepsilon}_{cr} = C_1 \sigma^{C_2} \varepsilon^{C_3} e^{-C_4/T} \tag{5}$$

where C_1, C_2, C_3, and C_4 are all material constants, which are measured according to the material creep test.

By introducing the Bailey's law as time function based on Equation (2) [29], the Norton–Bailey model (Equation (6)) under constant temperature can be derived, which can describe both the primary and secondary phases of creep:

$$\varepsilon_{cr} = A \sigma^n t^m \tag{6}$$

where m represents the material constants.

The strain rate form of the Norton–Bailey model can be obtained by taking the time derivative of Equation (6), which also corresponds to the time hardening model:

$$\dot{\varepsilon}_{cr} = Am \sigma^n t^{m-1} \tag{7}$$

The strain hardening model can be obtained by combining Equations (6) and (7) and eliminating the variable 't':

$$\dot{\varepsilon}_{cr} = A^{1/m} m \sigma^{n/m} \varepsilon^{(m-1)/m} \tag{8}$$

The Norton–Bailey model (time hardening model) and strain hardening model, shown in Equations (7) and (8), respectively, represent the forms of the models in Equations (4) and (5) under constant temperature conditions. This series of creep constitutive models, based on the Norton power law, has been widely applied in structural creep behavior analysis [33–35].

The Graham creep model (Equation (9)) is more complex than the Norton model, involving eight material parameters, and can describe all three phases of creep. Each phase consists of three (Norton–Bailey type) creep strain terms, providing higher accuracy and applicability [36–39].

$$\dot{\varepsilon}_{cr} = b_1 \sigma^{b_2} (t^{b_3} + b_4 t^{b_5} + b_6 t^{b_7}) e^{-b_8/T} \tag{9}$$

where $b_i (i \in \{1, 2, \cdots, 8\})$ is material constant.

In the study of the creep behavior of pressure hulls, Hou [40] proposed a numerical simulation method for creep damage evolution by combining the Norton model with the continuum damage mechanics, successfully simulating the creep damage evolution in a V-notch plate structure. Jiao et al. [41] and Li [42] applied the Norton–Bailey model to evaluate the creep strain rate of titanium alloy pressure hulls. By incorporating the creep ductility depletion model, a formula for multiaxial creep damage accumulation was derived. Zhao [43] utilized the Norton–Bailey model to fit the creep parameters of PMMA, the material used for observation windows. Zhao highlighted that the traditional single-parameter time-hardening creep model struggles to fully capture the complexities

of various working conditions. Consequently, an improved time-hardening model was proposed, considering the effects of ambient temperature and sustained stress levels.

Wang et al. [44] conducted a comparative analysis of the modified time-hardening model, the time-hardening model, and the Graham model. The modified time-hardening model (Equation (10)) is an inbuilt model in the finite element software Ansys, differing from Equation (4) in that the stress coefficient is subdivided into two separate coefficients. The study highlighted that the modified time-hardening model effectively characterizes the creep behavior of titanium alloy pressure structures during the primary and secondary creep phases, making it particularly suitable for the creep analysis of deep-sea titanium alloy pressure hulls. In contrast, the Graham model, despite its ability to capture all three creep phases, is hindered by its numerous parameters, leading to poor numerical convergence.

$$\dot{\varepsilon}_{cr} = \frac{C_1 \sigma^{C_2} t^{C_3+1} e^{-C_4/T}}{C_3 + 1} \tag{10}$$

Liu [45] applied the Norton–Bailey model to investigate the creep behavior and ultimate bearing capacity of a ring-stiffened cylindrical hull. The study indicated that the time-hardening model more accurately captures the variation of creep strain during the primary and secondary phases compared to the strain-hardening model, providing a better representation of structural behavior under creep. However, the time-hardening model exhibits limitations when addressing creep stress levels with large variations, requiring data grouping for effective curve fitting.

In summary, the Norton–Bailey model is the most widely used creep model in pressure hull research among the Norton model and its variants. It effectively describes the primary and secondary creep phases and, when combined with other models, can capture all three phases of creep. However, its adaptability is limited when fitting datasets with significant stress variations. Additionally, Ref. [45] highlighted that for titanium alloy creep tests at room temperature, only the primary and secondary phases occur within the experimental range, conforming to the Norton power law. This explains the prevalent use of the Norton–Bailey model in pressure hull creep studies.

Burger model and Findley model

In addition to the Norton model and its variants, the Findley model [46] (Equation (11)) and the Burger model [47] (Equation (12)) are commonly employed to predict the creep behavior of composite materials, particularly for the primary and secondary phases of creep. The Burger model integrates the Maxwell and Kelvin–Voigt models [48–50]: the first and third terms represent the instantaneous elastic strain and viscous strain from the Maxwell model, while the second term describes the viscoelastic deformation from the Kelvin–Voigt model [51].

$$\varepsilon_{cr} = \varepsilon_0 + At^n \tag{11}$$

$$\varepsilon_{cr} = \frac{\sigma}{E_M} + \frac{\sigma}{E_K(1 - e^{-E_K t/\eta_K})} + \frac{\sigma}{\eta_M} t \tag{12}$$

where ε_0 is the elastic strain, independent of time, which can be obtained by dividing the applied stress by the elastic modulus ($\varepsilon_0 = \sigma/E$) [52], E_M is the elastic modulus of Maxwell model, E_K is the elastic modulus of Kelvin model, and η_M and η_K are the viscosity of Maxwell and Kelvin models, respectively.

The Findley and Burger models are extensively applied in studying the creep behavior of viscoelastic materials [52–55]. Studies [56] have shown that both models effectively describe the creep behavior of carbon fiber composites, with the Findley model offering higher computational efficiency. Almeida et al. [57] demonstrated that the Findley model provides superior fitting performance at elevated temperatures compared to the Burger model, which is more suitable for detailed constitutive analysis. Liu et al. [13] employed

the Burger model to investigate the creep initiation, growth, and acceleration phases of PMMA used in pressure hull windows. Xu et al. [58] validated the Findley model's ability to accurately capture the viscoelastic behavior of PMMA in creep tests on acrylic glass cylindrical pressure hulls.

Both the Findley and Burger models exhibit high accuracy in describing the creep behavior of viscoelastic materials. However, the Findley model generally outperforms the Burger model in terms of simplicity and computational efficiency.

For a clearer comparison of the characteristics and applicability of the aforementioned creep models, their details are summarized in Table 1 for reference.

Table 1. Comparison of creep constitutive models

Model	Equation	Application	Characteristic
Norton	$\dot{\varepsilon}_{cr} = A\sigma^n$	The secondary creep phase	
Norton (General form)	$\dot{\varepsilon}_{cr} = C_1\sigma^{C_2}e^{-C_3/T}$	The secondary creep phase	
Time-hardening	$\dot{\varepsilon}_{cr} = C_1\sigma^{C_2}t^{C_3}e^{-C_4/T}$	The primary creep phase	
Strain-hardening	$\dot{\varepsilon}_{cr} = C_1\sigma^{C_2}\varepsilon^{C_3}e^{-C_4/T}$	The primary creep phase	
Norton–Bailey	$\dot{\varepsilon}_{cr} = Am\sigma^n t^{m-1}$	The primary and secondary creep phase	The model aligns with the creep behavior of titanium alloys but demonstrates limited adaptability to datasets involving significant stress variations [45], making it challenging to describe complex working conditions [43].
Strain-hardening (Constant temperature)	$\dot{\varepsilon}_{cr} = A^{1/m}m\sigma^{n/m}\varepsilon^{(m-1)/m}$	The primary creep phase	
Time-hardening (Modified)	$\dot{\varepsilon}_{cr} = \frac{C_1\sigma^{C_2}t^{C_3+1}e^{-C_4/T}}{C_3+1}$	The primary and secondary creep phase	
Graham	$\dot{\varepsilon}_{cr} = b_1\sigma^{b_2}(t^{b_3} + b_4t^{b_5} + b_6t^{b_7})e^{-b_8/T}$	All three phases of creep	It achieves higher fitting accuracy under elevated temperature conditions compared to the Norton–Bailey model [36], but the large number of parameters may impede the convergence of creep numerical calculations [44].
Findley	$\varepsilon_a = \varepsilon_0 + At^n$	The primary and secondary creep phase	It is suitable for viscoelastic materials and exhibits strong fitting performance at high temperatures.
Burger	$\varepsilon_{cr} = \frac{\sigma}{E_M} + \frac{\sigma}{E_K(1-e^{-E_Kt/\eta_K})} + \frac{\sigma}{\eta_M}t$	The primary and secondary creep phase	It is suitable for viscoelastic materials.

3.2. Modified Creep Constitutive Model

The commonly used uniaxial creep models discussed above cannot fully capture the creep behavior of all materials. To address this, parameters such as temperature and time are incorporated into the models based on material creep test results, enabling a more comprehensive consideration of multiple influencing factors. Through these adjustments, the modified models can more accurately represent the creep behavior and trends of materials.

Wang et al. [19] conducted a series of creep tests on scaled spherical pressure hull models and introduced a creep critical stress to modify the Norton model, yielding an improved creep model (Equation (13)) based on experimental data. Similarly, Golan et al. [59] applied this form of the creep model to describe the creep behavior of nickel-based alloys, demonstrating its applicability across different materials.

$$\dot{\varepsilon}_s = A(\sigma - \sigma_0)^m \tag{13}$$

He et al. [60] proposed an improved temperature-dependent time-hardening model (Equation (14)) for PMMA materials used in pressure hull observation windows. In this model, temperature effects were incorporated through higher-order polynomial terms. Test results demonstrated a goodness of fit of 0.95, resulting in a creep model applicable to various temperature conditions under uniaxial stress. Similarly, Zhao [43] employed this creep model to analyze and simulate the creep behavior of PMMA materials, further validating its effectiveness.

$$\dot{\varepsilon}_{cr} = \left(a_1 T^3 + b_1 T^2 + c_1 T + k_1 \sigma + d_1\right) \cdot \sigma^n t^{\left(a_2 T^2 + b_2 T + k_2 \sigma + c_2\right)} \tag{14}$$

Modifying uniaxial creep constitutive models improves their fit to experimental data and provides guidance for model selection. For materials mainly exhibiting steady-state creep, introducing critical yield stress reduces fitting errors. For materials significantly affected by temperature and time, incorporating temperature-related parameters enables a more accurate description of creep behavior. These modifications are essential for precise numerical simulation and prediction of material creep.

3.3. Multiaxial Creep Constitutive Model

In complex working environments, structures often endure multidirectional loads, resulting in multiaxial stress states. For instance, cylindrical pressure hulls in deep-sea environments experience both axial and circumferential compressive loads, while stress distributions in irregularly shaped hulls are even more intricate. Consequently, uniaxial creep models may fail to accurately capture the actual creep behavior of these structures. To address this, extensive research has been conducted on multiaxial creep in structural systems.

Current theoretical research on multiaxial creep models can be broadly categorized into two approaches [61]: the microscopic mechanism method based on void growth theory and the macroscopic phenomenological method based on extrapolation techniques and the theory of continuous damage mechanics (CDMs) [62–66]. The void growth theory describes the microscopic mechanism of fracture caused by the gradual nucleation, expansion, and final aggregation of internal microvoids due to stress during plastic deformation or creep of materials. The CDM quantifies the global accumulation of internal defects in materials by introducing damage variables (such as D or ω). The CDM-based method has gained significant attention due to its ability to simulate damage evolution via numerical calculations, especially with advancements in computational power. By incorporating parameters such as damage variables and equivalent stress, this method extends uniaxial creep constitutive models to account for the effects of multiaxial stress [67,68].

For instance, Zhu et al. [69] constructed a multiaxial creep constitutive model by extending the Norton model. This was achieved through the incorporation of multiaxial stress parameters and damage variables:

$$\begin{cases} \dot{\varepsilon}_{cr} = B(\frac{\sigma_e}{1-\omega})^n \\ \dot{\omega} = M\frac{\sigma_{rep}^{\chi}}{(1-\omega)^{\varphi}} \end{cases} \tag{15}$$

$$\sigma_e = \sigma_{\mathrm{VM}} = \sqrt{\frac{(\sigma_1-\sigma_2)^2-(\sigma_2-\sigma_3)^2-(\sigma_3-\sigma_1)^2}{2}} \tag{16}$$

$$\sigma_{rep} = \alpha\sigma_1 + (1-\alpha)\sigma_{VM} \tag{17}$$

where B, n, M, χ, and φ are the parameters related to the material, σ_e is the equivalent stress, σ_{rep} is the reference stress, $\omega \in [0,1]$ is the damage variable, where when $\omega = 1$, the material fails, σ_{VM} is the Von Mises equivalent stress, σ_1, σ_2, and σ_3 are the first, second, and third principal stress, respectively, the reference stress is represented by Equation (17) using the combination of the maximum principal stress and σ_{VM}, and $\alpha \in (0,1)$ is the combination coefficient.

Currently, research on the multiaxial creep behavior of pressure hulls is limited and primarily focuses on macroscopic phenomenological methods. Jiao et al. [41] and Li [42] utilized the Norton–Bailey model (Equation (7)) in conjunction with the ductility exhaustion model to derive a multiaxial creep damage accumulation equation for multispherical pressure hulls:

$$\dot{D}_c = \frac{\dot{\varepsilon}_{eq}^c}{\varepsilon_f^*} = \frac{Am\sigma^n t^{m-1}}{\varepsilon_f^*} \tag{18}$$

where $\dot{D}_c$ is the creep damage rate, $\dot{\varepsilon}_{eq}^c$ is the equivalent creep strain rate, ε_f^* is multiaxial creep ductility, $\dot{\varepsilon}_{eq}^c$ is determined by the Norton—Bailey model (Equation (7)), and ε_f^* is determined in different ways in Refs. [41,42].

Guo et al. [70,71] developed a tension–compression asymmetric multiaxial creep constitutive model for titanium alloy materials of pressure hulls. The model determines the constitutive matrix $\bar{R}_{pi}$ based on the stress state σ_p within the principal stress space and employs a linear transformation matrix Q to convert the principal stress space into the general stress space:

$$\dot{\varepsilon}_c = Q\bar{R}_{pi}Q^T\sigma \quad \text{if} \quad \sigma_p \in \Theta_i, i = 1,2,\cdots,8 \tag{19}$$

where σ is the stress vector, $\dot{\varepsilon}_c$ is the creep strain rate, Θ_i is the i^{th} subspace of principal stress space, $\bar{R}_{pi}$ is the creep constitutive matrix in the principal space, and Q is the coordinate transformation matrix.

The main space constitutive model $\bar{R}_{pi}$ incorporates the time hardening model to describe creep behavior under tension and the logarithmic model for compression:

$$\varepsilon_c = \begin{cases} A\sigma^n t^m, & \sigma > 0 \\ \alpha_1 \ln(\alpha_2 t + 1), & \sigma \le 0 \end{cases} \tag{20}$$

where ε_c is uniaxial creep strain, A, n, m, α_1 and α_2 are the material constants.

Currently, pressure hulls primarily use metallic materials, especially titanium alloys, and are typically spherical or cylindrical in shape. For these structures, the uniaxial creep model is sufficient to accurately describe their creep behavior. However, with the trend toward lighter pressure hulls and the increased use of composite materials, as well as the development of special-shaped pressure hulls, there is a growing need for more advanced research into multiaxial creep behavior. This will be crucial for understanding the complex

stress states in such structures and improving the accuracy of creep predictions under varied loading conditions.

4. Numerical Simulation of Creep

With the advancement of creep testing and the development of constitutive models, numerical methods have become a powerful tool for simulating the creep behavior of materials and structures. These methods allow for a deeper understanding of the creep deformation mechanism, including the behavior under complex stress states, providing a scientific foundation for engineering design and safety assessments. Currently, numerical simulations of pressure hull creep behavior predominantly utilize commercial finite element software such as Abaqus and Ansys. This section reviews the existing numerical simulation research on pressure hull creep and briefly introduces the multiscale analysis approach for studying the creep of pressure hulls.

4.1. Creep Simulation of Pressure Hulls

Commercial finite element software such as Abaqus and Ansys include built-in uniaxial creep models and secondary development interfaces, allowing users to directly implement or write customized creep constitutive subroutines for structural creep analysis. Abaqus incorporates time hardening, strain hardening, and hyperbolic sine models. Ansys, in addition to the time hardening and strain hardening models, also features the Norton model, generalized Graham model, and generalized Garofalo model for creep simulations. These built-in models offer flexibility for users in analyzing and simulating the creep behavior of pressure hull structures.

Wang et al. [44] compared the applicability of different creep constitutive models available in Ansys and Abaqus, using the modified time hardening model, time hardening model, and generalized Graham model in Ansys to simulate the creep behavior of a ring-stiffened cylindrical hull. The results revealed that the generalized Graham model, due to its numerous parameters, caused poor convergence in creep calculations. Liu [45] employed the time hardening model in Abaqus to analyze the creep and ultimate bearing capacity of ring-stiffened cylindrical hull. Similarly, Xu et al. [58] and Guo et al. [70] used the Findley constitutive model and multiaxial creep constitutive model in Abaqus to investigate the nonlinear buckling of pressure hulls (see Figure 6).

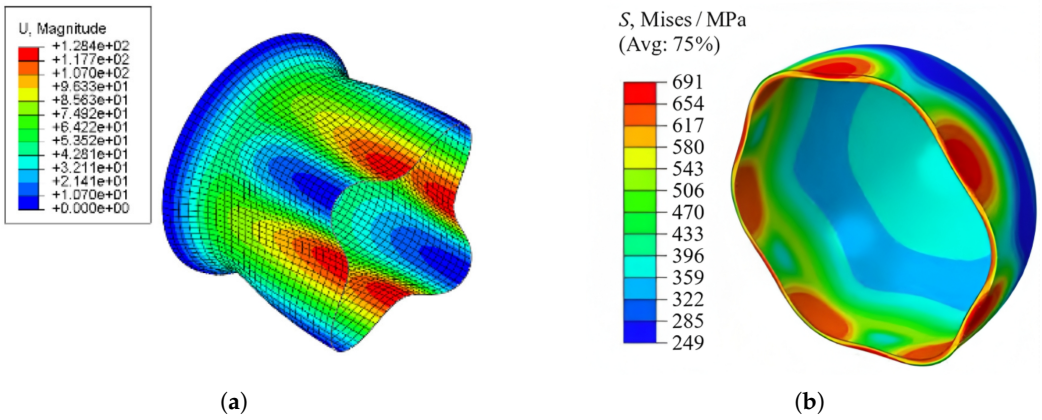


Figure 6. Nonlinear buckling of pressure hulls: (**a**) creep deformation of the model after 18 years of holding [58]; (**b**) equivalent stress distribution of the model after holding for 100 h [70].

When performing creep simulations in finite element software, the built-in uniaxial creep models may not always accurately represent the behavior of certain materials or structures, such as those significantly influenced by temperature or special-shaped pressure

hulls with complex multiaxial stress fields. In such cases, the secondary development functionality of the software becomes necessary. Ansys software offers the Ansys Parametric Design Language (APDL), allowing users to write custom programs for comprehensive finite element analysis. Abaqus, on the other hand, supports various subroutines such as UMAT and USDFLD for secondary development [12,27,36,41,72]. The UMAT subroutine is used to define complex material constitutive models, while USDFLD allows for the definition of custom field variables for boundary conditions, initialization, and output.

For example, Guo et al. from the Dalian University of Technology employed the UMAT subroutine to introduce a creep constitutive model that accounts for the tension–compression asymmetry of titanium alloy, enabling the numerical simulation of square plate torsion and Brazilian specimens [71]. Furthermore, they introduced a three-dimensional creep–fatigue damage model for titanium alloy pressure hulls using the USDFLD subroutine, successfully conducting a numerical analysis of a cone-cylinder pressure hull [73] (see Figure 7).

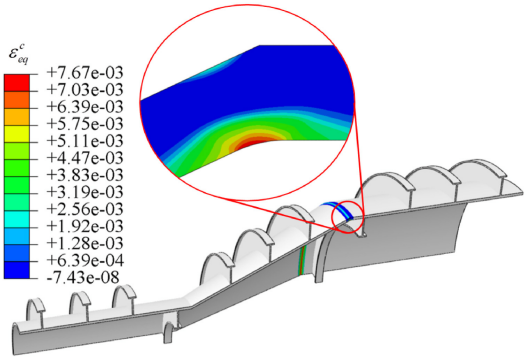


Figure 7. Equivalent creep strain distribution at the joint of the pressure hull after 2 h of holding load [73].

The above-mentioned method successfully enables the numerical simulation of structural creep behavior, but it has some limitations. Firstly, due to the complexity of the creep mechanism, which involves both macroscopic changes and the influence of the material's microstructure, these factors cannot be fully captured in the numerical model, potentially affecting the accuracy of the results. Secondly, most existing research focuses on the creep characteristics of isotropic materials, with a lack of studies on composite pressure hulls. Currently, the typical approach for analyzing the creep of composite laminates involves conducting creep tests, proposing a creep constitutive model, and validating the model through fitting test data or numerical simulations [57,74,75]. For different materials, especially when the layer parameters of composite materials vary, the creep parameters can differ significantly. As a result, elastic mechanics tests and tensile or compressive creep tests must be conducted for each variation to obtain the elastic constants (elastic modulus, shear modulus, and Poisson's ratio) and creep curves (strain–time curves). This leads to high testing costs, making the process less efficient and more resource-intensive. To overcome this, a multiscale approach can be employed to predict the performance parameters of composite materials without the need for extensive testing [76]. This approach will be discussed in more detail in the next section.

4.2. Multiscale Method of Composite Materials Creep Analysis

As a type of multiphase material, the mechanical properties and failure mechanisms of composites are influenced not only by macroscopic factors (such as boundary conditions, loads, and constraints) but also by microscopic characteristics (such as the properties of constituent phases, reinforcement shapes and distribution, and the interface between

the reinforcements and the matrix) [77,78]. Composite materials used in engineering involve both microscopic and macroscopic scales. While the structure typically ranges from centimeters to meters, the inclusion phase, such as particles and fibers, often spans the micrometer scale. To establish the relationship between microstructure, constituent material properties, and macroscopic behaviors, the multiscale method is required for composite materials.

In the field of fiber-reinforced composites, the multiscale method primarily involves modeling and calculating heterogeneous materials as globally homogeneous materials based on micromechanics. This approach is divided into two main methods: the analytical method and the micromechanics finite element method [77] (see Figure 8).

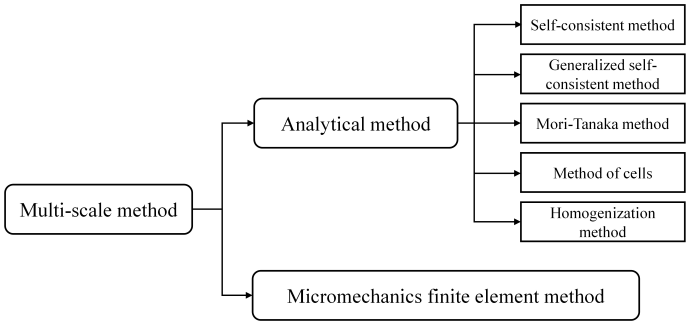


Figure 8. Multiscale method classification.

The analytical method includes several techniques such as the self-consistent method, generalized self-consistent method, Mori–Tanaka method, method of cells, and homogenization method. Classical micromechanics theories, such as the self-consistent method and Mori–Tanaka method, calculate material properties by averaging the strain and stress fields of representative elements. Method of cells utilizes the periodicity assumption of composite materials to divide the representative volume element (RVE) into several subcells for solving the basic equations of elastic mechanics. This leads to the determination of the stress–strain field within the RVE, and the macroscopic stress–strain relationship of the material is derived through homogenization theory. The homogenization method applies the theory to composites with periodic distribution, utilizing the energy principle, periodic conditions, and uniformity conditions to mathematically transform and simultaneously solve for the macroscopic material equivalent parameters. Recently, this method has been widely used to predict the properties of fiber-reinforced composites, with numerous calculation models being developed, including the Voigt model, Reuss model, and transversely isotropic averaging method [79–81]. The finite element method of micromechanics discretizes the structure by dividing the grid to obtain the stress–strain field, from which the macroscopic stress–strain relationship is derived using the homogenization method.

The multiscale method can significantly accelerate the modeling process for analyzing the creep characteristics of composite pressure hulls, reduce computational workload [77], and eliminate the need for material tests when composite material parameters change, thus saving both time and test costs [76]. It allows for the prediction of the effective properties of composite materials, such as elasticity, plasticity, and creep.

For elastic property prediction, Naili et al. [82] proposed a two-step homogenization (see Figure 9) scheme based on the finite element method. A model RVE is decomposed into unidirectional pseudo-grains (PG) where each PG is made of identical aligned fibers embedded in the matrix. The first step is to homogenize PG using mean-field (MF) homogenization methods, typically Mori–Tanaka. Next, in the second step, the RVE seen as an aggregate of PGs is homogenized with MF, typically a simple Voigt scheme. This

scheme is used to predict and compare the isothermal elastic properties of short fiber-reinforced composites.

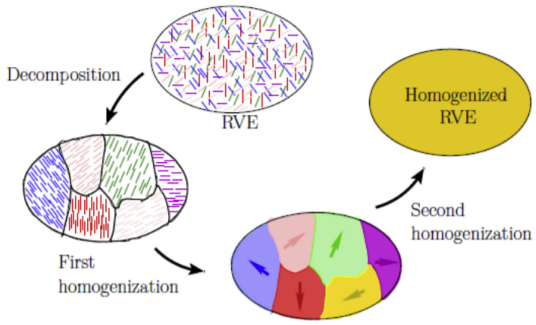


Figure 9. Two-step homogenization scheme [82].

Regarding plastic properties, Spilker et al. [83] introduced a mechanical model based on the Mori–Tanaka method, which predicted the elastic-plastic response of ceramic matrix composites while considering local damage. Wang [84] employed the homogenization method to explore the micro-plastic deformation mechanism of P92 steel. Ye [85] used the asymptotic homogenization theory to obtain the buckling load of the micro-scale finite element model, and combined this with the surrogate model to optimize the variable stiffness composite material.

For creep properties, Zhang [86] applied the Reuss model homogenization method in conjunction with polycrystalline plastic parameters to predict and analyze the creep properties of P91 steel. Xiao et al. [87] used the analytical method to simplify the complex stress state of the RVE into a simpler form and deduced the relationship between the creep displacement of flat cylinder indentation and time under constant load conditions to predict the creep behavior of zinc alloy ZA27. Katouzian et al. [88,89] used the homogenization method and finite element method to predict the creep behavior of carbon-fiber-reinforced composites, accounting for the transversely isotropic characteristics of unidirectional fiber composites in the vertical plane of the fibers, and performed experimental verification.

Based on the existing technical theories, this paper proposes a method for studying the creep properties of composite pressure hulls using the method of cell in the multiscale approach, as illustrated in Figure 10. Using fiber-reinforced resin matrix composites as an example, the process begins by defining the geometric size of RVE, fiber volume fraction, and material parameters of each component, such as elastic modulus, shear modulus, and Poisson ratio. Next, the average stress and strain in each principal direction are calculated through the homogenization method to determine the equivalent flexibility matrix and other equivalent mechanical parameters of the RVE. The creep parameters of the materials are then calculated using a theoretical creep model. Finally, structural creep is simulated based on the equivalent mechanical parameters derived from the homogenized material properties. Once the accuracy of the multiscale method is verified by experimental data, it can be applied to calculate the creep behavior of composite materials with varying ply parameters. This approach provides a more efficient and cost-effective way to predict and analyze the creep performance of composite pressure hulls under different conditions.

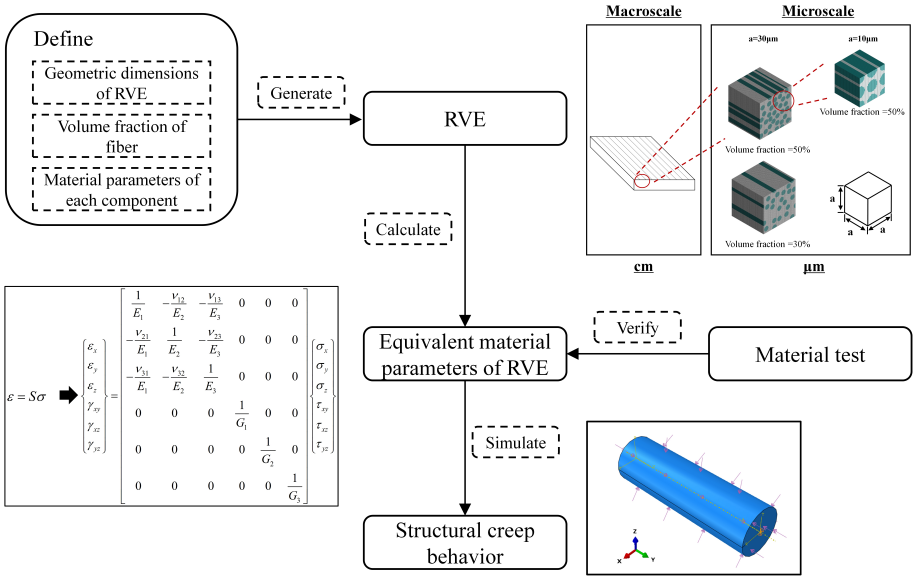


Figure 10. Numerical simulation method.

5. Conclusions

This paper reviews current creep studies on pressure hulls, focusing on three aspects: creep testing, creep constitutive modeling, and creep numerical simulation.

In creep constitutive modeling, uniaxial creep models are commonly used to describe the creep behavior of pressure hulls, given the relatively simple stress fields in typical designs. However, for pressure hulls significantly affected by temperature or other environmental factors, modifications to these models are essential. Additionally, for hulls with complex geometries—such as multisphere designs—where stress fields become locally intricate, multiaxial creep constitutive models are required for accurate representation.

For numerical simulation of creep behavior in pressure hulls, user-defined subroutines in finite element software like Abaqus are commonly employed to implement complex creep constitutive models. Furthermore, the paper emphasizes multiscale analysis for composite pressure hulls, which enhances the prediction of creep parameters and boosts computational efficiency.

Drawing from challenges in existing literature, the paper proposes three research directions to advance the study of creep properties in composite pressure hulls:

1. Develop numerical methods to quantify and incorporate uncertainty in creep predictions for pressure hulls, addressing variability in environmental factors, material degradation, and fatigue;
2. Develop multiscale techniques to predict the creep behavior of high-performance composites, improving reliability in deep-sea environments with limited experimental data;
3. Integrate machine learning with multiscale analysis to accelerate predictions of composite creep performance, enhancing the efficiency of traditional design methods.

Author Contributions: Investigation, Y.Z., C.Y. and S.Y.; writing—original draft preparation, Y.Z., C.Y. and S.Y.; writing—review and editing, Y.Z., C.Y. and S.Y.; funding acquisition, C.Y. All authors have read and agreed to the published version of the manuscript.

Funding: This research was funded by the Key Research and Development Plan of Shandong Province (No. 2024CXGC010807).

Data Availability Statement: No new data were created or analyzed in this study.

Conflicts of Interest: The authors declare no conflicts of interest.

References

1. Yang, R.; Ma, Y. Status and Prospect of Key Materials for Deep Submergence Facilities. *Sci. Technol. Foresight* **2022**, *1*, 145–156. (In Chinese)
2. *ASTM E139-11*; Standard Test Methods for Conducting Creep, Creep-Rupture, and Stress-Rupture Tests of Metallic Materials. ASTM: West Conshohocken, PA, USA, 2018. [CrossRef]
3. *ASTM D2990-17*; Standard Test Methods for Tensile, Compressive, and Flexural Creep and Creep-Rupture of Plastics, ASTM: West Conshohocken, PA, USA, 2017. [CrossRef]
4. Yan, Y.; Liu, P.; Wang, A.; Xie, J.; Bian, X.; Wang, Z. Investigation on the Room Temperature Compressive Creep Behavior of TC4 Titanium Alloy Joints with Vacuum Electron Beam Welding. *Solid State Commun.* **2024**, *391*, 115641. [CrossRef]
5. Wang, K.; Gao, L.; Zhang, S.; Huang, X. Experimental Investigations on Tensile Creep of New Titanium Alloy Materials at Room Temperature. *J. Ship Mech.* **2022**, *26*, 557–565. (In Chinese)
6. Yan, S.C.; Wu, Y.K.; Shang, L.; Ren, J.Q.; Zhang, Y.M.; Xin, C.; Wang, Q.; Ai, T.T. Compressive Creep Damage of Ti–6Al–4V ELI Alloy with Bimodal Structure at Room Temperature. *J. Mater. Res. Technol.* **2024**, *33*, 4899–4907. [CrossRef]
7. Xi, G. Studies on Room Temperature Creep and Dwell Fatigue Properties of Marine Engineering Titanium Alloys. Ph.D. Thesis, University of Science and Technology of China, Hefei, China, 2021. (In Chinese) [CrossRef]
8. *GB/T 2039-2024*; Metallic Materials-Uniaxial Creep Testing Method in Tension. National Standard of the People's Republic of China: Beijing, China, 2024.
9. *GB/T 15048-94*; Cellular Plastics, Rigid-Determination of Compressive Creep. National Standard of the People's Republic of China: Beijing, China, 1994.
10. *ASTM E8/E8M-21*; Standard Test Methods for Tension Testing of Metallic Materials. ASTM: West Conshohocken, PA, USA, 2021.
11. Chen, J. Study on Creep Recovery Characteristics of New Titanium Alloy at Room Temperature and Influence of Load Protection-Fatigue Crack Growth Behavior. Master's Thesis, Jiangsu University of Science and Technology, Zhenjiang, China, 2023. (In Chinese) [CrossRef]
12. Liu, Z.; Wang, F.; Zhao, B.; Zhang, J.; Gaidai, O.; Sun, Z.; Wang, K. Room-Temperature Creep Deformation of a Pressure-Resistant Cylindrical Structure Made of Dissimilar Titanium Alloys. *J. Mar. Sci. Eng.* **2024**, *12*, 1419. [CrossRef]
13. Liu, P.; Li, J.; Wang, S.; Leng, J. Finite Element Analysis of Viscoelastic Creep Behaviors of Deep-Sea Manned Submersible Viewport Windows. *Int. J. Press. Vessel. Pip.* **2020**, *188*, 104218. [CrossRef]
14. Slaughter, W.S.; Fleck, N.A.; Budiansky, B. Compressive Failure of Fiber Composites: The Roles of Multiaxial Loading and Creep. *J. Eng. Mater. Technol.* **1993**, *115*, 308–313. [CrossRef]
15. Guedes, R.; Vaz, M.; Ferreira, F.; Morais, J.L. Response of CFRP Laminates under High Strain Rate Compression until Failure. *Sci. Eng. Compos. Mater.* **2005**, *12*, 145–152. [CrossRef]
16. Kong, F. Study on Fatigue—Creep Properties of Carbon Fiber Reinforced Composite. Master's Thesis, Civil Aviation University of China, Tianjing, China, 2022. (In Chinese) [CrossRef]
17. Lv, J.; Xiao, Y.; Zhou, Y.; Xie, Y. Characterization and Modeling of the Creep Behavior of Fiber Composites with Tension and Compression Asymmetry. *Int. J. Mech. Sci.* **2020**, *170*, 105340. [CrossRef]
18. Jiang, X.; Yu, C.; Li, Y.; Zeng, Y. Ultimate State Assessment of Medium-Thick Composite Cylindrical Pressure Shells Based on Progressive Damage. *Ocean Eng.* **2023**, *289*, 116128. [CrossRef]
19. Wang, L.; Li, Y.; Sun, C.; Qiu, J.; Huang, J.; Jiang, X.; Sun, Z.; Wan, Z. Compressive Creep Behavior of Spherical Pressure Hull Scale Model for Full-Ocean-Depth Manned Submersible. *Ocean Eng.* **2022**, *266*, 112831. [CrossRef]
20. Stachiw, J.D.; Clark, A.; Brenn, C.B. Acrylic Plastic Spherical Pressure Hull for 2439 m (8000 Ft) Design Depth: Phase I. *J. Energy Resour. Technol.* **1987**, *109*, 40–47. [CrossRef]
21. Swindeman, R.; Swindeman, M. A Comparison of Creep Models for Nickel Base Alloys for Advanced Energy Systems. *Int. J. Press. Vessel. Pip.* **2008**, *85*, 72–79. [CrossRef]
22. Bellieud, M. Homogenization of Norton–Hoff Fibered Composites with High Viscosity Contrast. *SIAM J. Math. Anal.* **2022**, *54*, 649–692. [CrossRef]
23. Sattar, M.; Othman, A.R.; Akhtar, M.; Kamaruddin, S.; Khan, R.; Masood, F.; Alam, M.A.; Azeem, M.; Mohsin, S. Curve Fitting for Damage Evolution through Regression Analysis for the Kachanov-Rabotnov Model to the Norton-Bailey Creep Law of SS-316 Material. *Materials* **2021**, *14*, 5518. [CrossRef]
24. Sithickbasha, A.A.; Mahesh, S. The Role of the Constitutive Model in Creep Crack Growth Modelling. *Eng. Fract. Mech.* **2015**, *150*, 47–57. [CrossRef]
25. Hyde, T.H.; Jones, I.A.; Peravali, S.; Sun, W.; Wang, J.G.; Leen, S.B. Anisotropic Creep Behaviour of Bridgman Notch Specimens. *Proc. Inst. Mech. Eng. Part L J. Mater. Des. Appl.* **2005**, *219*, 163–175. [CrossRef]
26. Arbel, A. Estimating Creep Rates during Tensile Cyclic Loading. *J. Test. Eval.* **1997**, *25*, 358–361. [CrossRef]
27. Jamil, A.; Varshney, V. A User-Defined Subroutine for Numerical Modelling of Failure Due to Creep under Compression in Carbon Fibre Reinforced Composite Materials. *Mater. Res. Express* **2019**, *6*, 085609. [CrossRef]

28. Norton, F.H. *The Creep of Steel at High Temperatures*; McGraw-Hill: New York, NY, USA, 1929.
29. Bailey, R.W. The Utilization of Creep Test Data in Engineering Design. *Proc. Inst. Mech. Eng.* **1935**, *131*, 131–349. [CrossRef]
30. Graham, A.; Walles, K.F.A. Relation between Long and Short Time Properties of a Commercial Alloy. *J. Lron Steel Inst.* **1955**, *179*, 105–120.
31. Garofalo, F.; Butrymowicz, D.B. Fundamentals of Creep and Creep-Rupture in Metals. *Phys. Today* **1966**, *19*, 100–102. [CrossRef]
32. Wang, X. Research and Application of High Temperature Creep Theory Model and Numerical Simulation for Uns N10003 Alloy. Ph.D. Thesis, Shanghai Institute of Applied Physics, Chinese Academy of Sciences, Shanghai, China, 2018. (In Chinese)
33. Gebrehiwot, S.Z.; Espinosa-Leal, L.; Linderbäck, P.; Remes, H. Experimental Investigation and Modelling of the Nonlinear Creep Behaviour of Additive-Manufactured Carbon Fibre-Reinforced Polyethylene Terephthalate (CF-PET). *Compos. Part C Open Access* **2024**, *15*, 100530. [CrossRef]
34. Dong, S.; Gong, Z.; Chen, Z.; Qu, Y.; Chen, R.; Liu, S.; Li, G. High Temperature Tensile Creep Behavior and Microstructure Evolution of Ti60 Alloy Rolled Sheet. *Mater. Today Commun.* **2024**, *41*, 110805. [CrossRef]
35. Lin, L.; Zhao, S.; Zheng, T.; Lin, Y.; Chen, N.Z.; Zhang, J. Fatigue Assessment for Tower Bolts of Floating Offshore Wind Turbine Considering Preload Loss Due to Ambient Temperature Creep. *Ocean Eng.* **2024**, *313*, 119527. [CrossRef]
36. Shi, J.; Qiang, B.; Xie, Y.; Xie, Q.; Liu, X. Determination of Creep Behavior of Vessel Steel Q345R at Elevated Temperatures. *Int. J. Press. Vessel. Pip.* **2024**, *211*, 105273. [CrossRef]
37. He, L.; Zhang, B.; Zhou, L. Influence of Creep Constitutive Models for an AlSiCu Alloy on Load Distribution of Bolted Joint. *Eng. Fail. Anal.* **2021**, *128*, 105627. [CrossRef]
38. Fehér, A.; Linn, S.; Schwienheer, M.; Scholz, A.; Berger, C. An Interactive Approach to Creep Behavior Modeling. *Mater. Sci. Eng. A* **2009**, *510–511*, 29–34. [CrossRef]
39. Rojas-Ulloa, C.; Morch, H.; Tuninetti, V.; Duchêne, L.; Habraken, A.M. Implementation of a Modified Graham-Walles Viscosity Function within a Chaboche Viscoplastic Constitutive Model. *Comput. Math. Appl.* **2024**, *155*, 165–175. [CrossRef]
40. Hou, J. Study on Method of Evaluating the Creep Fatigue Damage and Life for Submersible Pressure Shell. Master's Thesis, Dalian University of Technology, Dalian, China, 2020. (In Chinese) [CrossRef]
41. Jiao, T.; Liu, G.; Guo, Y.; Li, Y.; Hu, X.; Zhang, H. Study on Cold Creep-Fatigue Characteristics of Pressure-resistant Shells with Multi-sphere Junction for Deep-sea Submersibles. *Shipbuild. China* **2023**, *64*, 157–168. (In Chinese)
42. Li, Y. Research on Fatigue-Creep Damage and Life Prediction of Pressure Hull. Master's Thesis, Dalian University of Technology, Dalian, China, 2023. (In Chinese) [CrossRef]
43. Zhao, B. Failure Mechanism Study for the Windows of the Deep-Sea Human Occupied Vehicle. Ph.D. Thesis, Jimei University, Xiamen, China, 2024. (In Chinese) [CrossRef]
44. Wang, L.; Qu, P.; Huang, J.; Zhang, A.; Wan, Z. Creep Numerical Calculation Methods and Test Verification for Pressure Structures of Titanium Alloy. *J. Ship Mech.* **2019**, *23*, 190–199. (In Chinese)
45. Liu, D. Study on Creep Properties of Titanium Alloy Ring Ribbed Cylindrical Shell Under Deep Sea Pressure. Master's Thesis, Harbin Engineering University, Harbin, China, 2023. (In Chinese) [CrossRef]
46. Findley, W.N.; Davis, F.A. *Creep and Relaxation of Nonlinear Viscoelastic Materials*; Courier Corporation: North Chelmsford, MA, USA, 2013.
47. Faraz, M.; Besseling, N.; Korobko, A.; Picken, S. Characterization and Modeling of Creep Behavior of a Thermoset Nanocomposite. *Polym. Compos.* **2015**, *36*, 322–329. [CrossRef]
48. Liang, Y.; Guan, P. Improved Maxwell Model with Structural Dashpot for Characterization of Ultraslow Creep in Concrete. *Constr. Build. Mater.* **2022**, *329*, 127181. [CrossRef]
49. Liu, C.; Liu, X.; Zhang, X.; Wang, Y. Improved Unsteady Maxwell Rock Creep Model and Parameter Identificatio. *China Rural. Water Hydropower* **2024**, 1–10. (In Chinese)
50. Fliegener, S.; Hohe, J. An Anisotropic Creep Model for Continuously and Discontinuously Fiber Reinforced Thermoplastics. *Compos. Sci. Technol.* **2020**, *194*, 108168. [CrossRef]
51. Militký, J.; Jabbar, A. Comparative Evaluation of Fiber Treatments on the Creep Behavior of Jute/Green Epoxy Composites. *Compos. Part B Eng.* **2015**, *80*, 361–368. [CrossRef]
52. Amir, A.L.; Ishak, M.R.; Yidris, N.; Mohd Zuhri, M.Y.; Asyraf, M.R.M.; Razman, M.R.; Ramli, Z. Full-Scale Evaluation of Creep Coefficients and Viscoelastic Moduli in Honeycomb Sandwich Pultruded GFRP Composite Cross-Arms: Experimental and Numerical Study. *Results Eng.* **2024**, *21*, 101850. [CrossRef]
53. Karabal, M.; Yıldız, A. Creep Resistance Enhancement and Modeling of 3D Printed Polyetherimide/Carbon Black Composites. *Compos. Struct.* **2024**, *345*, 118398. [CrossRef]
54. Yang, Y. A Study of Creep Behavior of Carbon Fiber Reinforced Polypropylene Composites. Master's Thesis, Donghua University, Shanghai, China, 2023. (In Chinese) [CrossRef]
55. Li, J.; Liu, Z.; Liu, M.; Kuang, Y.; Zhang, Z.; Chen, X. Temperature-Dependent Creep Damage Mechanism and Prediction Model of Fiber-Reinforced Phenolic Resin Composites. *Int. J. Mech. Sci.* **2024**, *278*, 109477. [CrossRef]

56. Zhang, Y.; Lu, Q.; Li, x.; Zhu, S. Considering the Influence of Temperature and Stress Levels on the Nonlinear Creep Model of Gfrp in a Water Environment. *Acta Mater. Compos. Sin.* **2024**, *24*, 1–9. (In Chinese) [CrossRef]
57. Almeida, J.H.S.; Ornaghi, H.L.; Lorandi, N.P.; Bregolin, B.P.; Amico, S.C. Creep and Interfacial Behavior of Carbon Fiber Reinforced Epoxy Filament Wound Laminates. *Polym. Compos.* **2018**, *39*, E2199–E2206. [CrossRef]
58. Xu, S.; Gao, H.; Qiu, P.; Shen, W.; Cai, Y.; Liu, D. Stability Analysis of Acrylic Glass Pressure Cylindrical Shell Considering Creep Effect. *Thin Walled Struct.* **2022**, *181*, 110033. [CrossRef]
59. Golan, O.; Arbel, A.; Eliezer, D.; Moreno, D. The Applicability of Norton's Creep Power Law and Its Modified Version to a Single-Crystal Superalloy Type CMSX-2. *Mater. Sci. Eng. A* **1996**, *216*, 125–130. [CrossRef]
60. He, Z.; Wang, F.; Wang, H.; Zhao, B. Parametric Analysis on Creep Deformation of Deep-Sea PMMA Observation Window. *Appl. Sci.* **2024**, *14*, 1040. [CrossRef]
61. Lan, X. Research on Influence of Multiaxial Creep on Life of Key Components in Ultra-Supercritical Units. Ph.D. Thesis, North China Electric Power University, Beijing, China, 2018. (In Chinese)
62. Alang, N.; Nikbin, K. A New Approach to Predict Creep Rupture of Grade 92 Steel Under Multiaxial Stress States. *Int. J. Mech. Sci.* **2019**, *163*, 105096. [CrossRef]
63. Nikbin, K. A Unified Multiscale Ductility Exhaustion Based Approach to Predict Uniaxial, Multiaxial Creep Rupture and Crack Growth. *Eng. Fract. Mech.* **2017**, *179*, 240–259. [CrossRef]
64. Zhang, K.; Tan, J.P.; Sun, W.; Nikbin, K.; Tu, S.T. Determination of Multiaxial Stress Rupture Criteria for Creeping Materials: A Critical Analysis of Different Approaches. *J. Mater. Sci. Technol.* **2023**, *137*, 14–25. [CrossRef]
65. Zhang, K.; Zhu, W.B.; Tan, J.P.; Zhang, Y.C.; Zhang, C.C.; Gong, C.Y.; Zhang, X.C.; Tu, S.T. Equivalent Conversion of Different Multiaxial Stress Rupture Criteria for Creep Materials Based on Skeletal Point Stresses. *Eng. Fract. Mech.* **2024**, *310*, 110439. [CrossRef]
66. Yao, H.; Xuan, F.; Wang, Z.; Tu, S. Multi-Axial Creep Design Models Based on the Cavity Growth Theory and Its Applications in Engineering. *Nucl. Power Eng.* **2007**, *28*, 72–77. (In Chinese)
67. Zhang, Y. Creep Damage and Crack Growth Analysis of the Brazed Joint Under Multi-Axial Stress State. Ph.D. Thesis, East China University of Science and Technology, Shanghai, China, 2016. (In Chinese)
68. Chang, Y. Research on Creep Damage and Microstructual Evolution of Power Station Components Under Complex Stress States. Ph.D. Thesis, North China Electric Power University, Shanghai, China, 2017. (In Chinese)
69. Zhu, J.; Wang, D.; Bao, S.; Zhou, Q.; Qin, Z.; Zhong, F.; Mao, J. Experimental and Numerical Study on Multiaxial Creep Behavior of 16MND5 Steel at 700 °C. *J. Nucl. Mater.* **2022**, *558*, 153387. [CrossRef]
70. Guo, Y.; Liu, G. Research on Assessment Method of Creep Buckling Strength of Titanium Alloy Pressure Shell for Deep-sea Submersible. *Shipbuild. China* **2024**, *65*, 25–36. (In Chinese)
71. Guo, Y.; Liu, G.; Huang, Y. A Complemented Multiaxial Creep Constitutive Model for Materials with Different Properties in Tension and Compression. *Eur. J. Mech. A/Solids* **2022**, *93*, 104510. [CrossRef]
72. He, Z.; Wang, F.; Li, Y. Analysis on Creep Deformation of Deep-Sea Fullytransparent Pressure-Resistant Hull (in Chinese). *Mech. Eng.* **2024**, *46*, 559–569.
73. Guo, Y.; Liu, G.; Xu, J.; Jiao, T. Numerical Analysis on the Creep-Fatigue Damage of Titanium Alloy Deep-Sea Pressure Hull at Room Temperature. *Mar. Struct.* **2024**, *96*, 103639. [CrossRef]
74. Nguyen, D.; Ogale, A. Compressive and Flexural Creep Behavior of Carbon Fiber/PEEK Composites. *J. Thermoplast. Compos. Mater.* **1991**, *4*, 83–99. [CrossRef]
75. Goertzen, W.K.; Kessler, M. Creep Behavior of Carbon Fiber/Epoxy Matrix Composites. *Mater. Sci. Eng. A* **2006**, *421*, 217–225. [CrossRef]
76. Antin, K.N.; Laukkanen, A.; Andersson, T.; Smyl, D.; Vilaça, P. A Multiscale Modelling Approach for Estimating the Effect of Defects in Unidirectional Carbon Fiber Reinforced Polymer Composites. *Materials* **2019**, *12*, 1885. [CrossRef]
77. Zheng, X.; Zheng, X.; Linhu, G. The Research Progress on Multiscale Method for the Mechanical Analysis of Composites. *Adv. Mech.* **2010**, *40*, 41–56. (In Chinese)
78. Shen, G.; Hu, G.; Liu, B. *Mechanics of Composite Materials*, 2nd ed.; Tsinghua University Press: Beijing, China, 2013. (In Chinese)
79. Barbero, E.J. *Finite Element Analysis of Composite Materials Using Abaqus®*; CRC Press: Boca Raton, FL, USA, 2023. [CrossRef]
80. Li, S. Study on the Multi-Scale and Refine Design of Composite Materials. Ph.D. Thesis, Hunan University, Changsha, China, 2023. (In Chinese) [CrossRef]
81. Zhou, J. Numerical Simulation Study of Macroscopic Material Constants of Short Fiber Reinforced Composites. Master's Thesis, Henan Polytechnic University, Jiaozuo, China, 2023. (In Chinese) [CrossRef]
82. Naili, C.; Doghri, I.; Kanit, T.; Sukiman, M.S.; Aissa-Berraies, A.; Imad, A. Short Fiber Reinforced Composites: Unbiased Full-Field Evaluation of Various Homogenization Methods in Elasticity. *Compos. Sci. Technol.* **2020**, *187*, 107942. [CrossRef]
83. Spilker, K.; Lebensohn, R.A.; Jacobsen, G.; Capolungo, L. A Mean Field Homogenization Model for the Mechanical Response of Ceramic Matrix Composites. *Compos. Struct.* **2025**, *352*, 118630. [CrossRef]

84. Wang, X. Crystal Plasticity Simulation Study on the Effect of Microstructure of P92 Steel on Mechanical Behavior. Master's Thesis, Tianjin University of Technology, Tianjin, China, 2022. (In Chinese) [CrossRef]
85. Ye, F. The Research on the Optimization and Design of Variable Stiffness Composite Material Based on the Surrogate Method. Ph.D. Thesis, Hunan University, Changsha, China, 2021. (In Chinese) [CrossRef]
86. Qijun, Z. Crystal Plasticity Based Micromechanical Simulation and Investigation of Creep for P91 Steels. Master's Thesis, Harbin Institute of Technology, Harbin, China, 2019. (In Chinese) [CrossRef]
87. Xiao, H.R.; Cai, L.X.; Han, G.Z. Semi-Analytical Creep Model to Obtain Norton's Law of Materials under Flat Indentation and Its Applications. *J. Mater. Res. Technol.* **2023**, *25*, 905–911. [CrossRef]
88. Katouzian, M.; Vlase, S.; Scutaru, M.L. Finite Element Method-Based Simulation Creep Behavior of Viscoelastic Carbon-Fiber Composite. *Polymers* **2021**, *13*, 1017. [CrossRef] [PubMed]
89. Katouzian, M.; Vlase, S. Creep Response of Carbon-Fiber-Reinforced Composite Using Homogenization Method. *Polymers* **2021**, *13*, 867. [CrossRef] [PubMed]

Disclaimer/Publisher's Note: The statements, opinions and data contained in all publications are solely those of the individual author(s) and contributor(s) and not of MDPI and/or the editor(s). MDPI and/or the editor(s) disclaim responsibility for any injury to people or property resulting from any ideas, methods, instructions or products referred to in the content.